Indian Journal of Natural Products and Resources
Vol. 15(4), December 2024, pp 535-545
DOI: 10.56042/ijnpr.v15i4.9645

Microencapsulation of *Citrus sinensis* peel extract using synthesised guar gum grafted acrylic acid superabsorbent polymer: Studies on sustainable release kinetics and antimicrobial activity

S B Shruthi* and G N Rameshaiah

Department of Chemical Engineering, B. M. S. College of Engineering Post box No. 19,
Bull Temple Road, Bengaluru 560019, Karnataka, India

Received 15 March 2024; revised received 27 August 2024; accepted 11 October 2024

Citrus sinensis peel, a major waste fraction of *C. sinensis* fruit, contains phytochemicals such as flavonoids, terpenoids, saponins, tannins, etc., which find application in the wide horizon. In order to protect an active component from physical and chemical reactions and retain its functional properties, microencapsulation is a technique that creates a functional barrier between core and shell material. This study tailored shell material to obtain guar gum grafted acrylic acid superabsorbent polymer (GG-g-AASAP) via microwave irradiated graft polymerisation. The effect of monomer (acrylic acid), initiator (Ammonium persulfate), crosslinker (methylene bis acrylamide), and reaction time on grafting percentage was evaluated and optimised. The GG-g-AA SAP was characterised by Fourier Transform Infrared (FTIR) spectroscopy and Scanning Electron Microscopy (SEM) to confirm the grafting of acrylic acid onto guar gum. The peel of *C. sinensis* was extracted using an aqueous extraction method with a yield percentage of 10.8%. Phytochemical qualitative analysis illustrates the presence of various phytochemicals like flavonoids, tannins, saponins, terpenoids, etc.; *C. sinensis* was encapsulated by coacervation phase separation method using synthesised GG-g-AA SAP, which resulted in the encapsulation efficiency of 76.8%. Release kinetics followed zero-order kinetics and the Korseymeyermodel, which approves super case II transport with sustainable release. Encapsulated *C. sinensis*is tested against a gram-negative bacteria, *Escherichia coli*, and a gram-positive bacteria, *Bacillus subtilis,* which exhibited antibacterial properties. The results depict a higher zone of inhibition for encapsulated *C. sinensis* than that without encapsulation. The study suggests that encapsulation has increased the antibacterial property of *C. sinensis* due to barrier protection from GG-g-AA SAP.

Keywords: Antimicrobial activity, *Citrus sinensis* peel extract, Microencapsulation, Release kinetics, Superabsorbent polymer

IPC code; Int. cl. (2021.01)− A61K 36/00, A61K 36/48, A61P 31/00

Introduction

Microencapsulation has proved to be an effective technique for protecting active ingredients. It is a method through which the core material is protected or covered by a continuous film called shell material. Microencapsulation finds application in various fields like food technology[1], cancer treatment[2], agriculture[3], pharmaceutical[4], home and personal care products[5], wastewater treatment[6] and many more. Many factors, such as the type of shell material, core material, technique applied for encapsulation, pH, etc., affect microencapsulation[7]. The type of shell material is of greater concern as non-biodegradable shell material, despite its benefits, has adverse effects on the environment. Non-biodegradable material such as high-density polyethylene is used as phase change material to fill the paraffin wax-based microencapsulated capsules. Though it exhibits a great plasticising effect upon copious usage, it leads to difficulty in disposal as it creates a hostile effect on the environment[8]. Low-density polyethylene film is used for laminating polyvinyl alcohol (PVA) encapsulated onto cinnamon oil which acts as insect-repellent[9]. Despite the benefits of the usage of non-biodegradable shell materials, the risk of damage in the longer run is countable. There comes a need for environmentally friendly shell material that can replace the former and provide similar benefits. Naturally available gums, starch, cellulose, etc., are thus modified for better stability and industrial versatility[10–12]. Various techniques of modification are applied to naturally available materials for industrial application, amongst which surface modification, functionalisation, and grafting are on the front line[13,14]. In this study, guar gum-based superabsorbent polymer is used as shell material and *C. sinensis* peel extract as core material.

*Correspondent author
Email: shruthisb@bmsce.ac.in

C. sinensis, has a wide variety of health benefits. According to the Food and Agricultural Organization of United Nations: Economic and Social Department: The Statistical Division, worldwide production of *C. sinensis* is 73,298,838 tons per annum. Brazil takes first, and India stands third place with 17,251,291 and 7,503,000 tons per annum, respectively[15]. *C. sinensis* waste comprises 50–60% w/w processed fruit, in which 60–65% w/w is of peels and 30–35% w/w is of internal tissue and seeds[16]. Waste management of this *C. sinensis* peel led to research that recognised its antioxidant properties and essential oils and phytochemicals like flavonoids, phenolic compounds, and terpenoids[17,18]. This initiated numerous sustainable solutions in various industries. The antioxidant property of *C. sinensis* peel extract has provided the benefit of corrosion inhibition of carbon steel in an acidic medium[19]. Volatile extract of *C. sinensis* peel exhibits insecticidal activity against mosquitoes, houseflies, and cockroaches[20]. *C. sinensis* peel extract manifests antimicrobial activity when tested against *Staphylococcus aureus, Enterococcus faecalis, Pseudomonas aeruginosa, Escherichia coli*, and *Salmonella typhimurium* bacterial strains, and *Candida albicans, Aspergillus niger* and *Penicillium notatum* fungal strains[21]. It is used in the green synthesis of zinc oxide nanoparticles with enhanced antibacterial activity[22]. Thus, protecting the active component plays an important role in better application.

Guar gum is an endosperm of guar or cluster bean plant (*Cyamopsis tetragonolobus*). It belongs to the *Leguminosae* family. Endosperm has galactomannan polysaccharide upon dissolving in water, forms hydrogen bonds and increases the viscosity significantly. It is readily soluble in water at room temperature and biodegradable, and hydrogen bonding phenomena make guar gum a desirable material as shell material[23]. Guargum-based hydrogels were synthesised, which exhibit biodegradable and anti bacterial properties[24]. Thimma *et al.* studied the complex coacervation of gelatin with sodium carboxymethyl guar gum, in which clove oil and sulphamethoxazole are microencapsulated[25]. Thus, guar gum proves to be one of the best natural polymers accustomed to hydrogel synthesis.

Recently, Ghasemi *et al.* deliberated the encapsulation of orange peel oil using whey protein pectin complex nanocomposites and its controlled release. The work exhibited 70-88% encapsulation efficiency under different temperatures from 30 to 90°C and pH 3,7, and 11[26]. Antioxidants from the orange peel were extracted using an ethanol solvent via ultrasound-assisted extraction, and they were encapsulated using an alginate-chitosan polymer composite by Savic *et al.* The release of phenols/antioxidants in the extremely acidic environment of gastric juice, kinetics followed the Fickian diffusion model[27]. The current study aims to synthesise the superabsorbent polymer (SAP) by grafting acrylic acid (monomer) onto the guar gum backbone via microwave irradiation. The synthesised SAP encapsulates the extracted *C. sinensis* peel extract (OPE). The novel product is subjected to an antibacterial test against *Escherichia coli* and *Bacillus subtilis* strains.

Further comparison of the antibacterial activity of SAP and SAP-e-OPE interprets that SAP developed antibacterial properties due to the presence of acrylic acid and OPE upon encapsulation with SAP, which has a higher rate of antibacterial properties. The present work finds a solution for using *C. sinensis* peels and, thus, follows the waste-to-wealth concept. Both shell and core are naturally available and biodegradable materials with twinning advantages, resulting in a potential product for biomedical application.

Materials and Methods

Chemical reagents

Guar gum, AksharchemIndia Ltd.; Glacial Acetic acid (Qualigens), NaOH pellets R(Qualigens), Methylene bis acrylamide (SDFCL), Ammonium per sulfate (SDFCL), Acetone (Qualigens), Ferric chloride anhydrous (SDFCL), copper sulphate pentahydrate (Sigma Aldrich), Benedict's reagent, chloroform (Qualigens), sulfuric acid (SDFCL), nutrient agar (HIMEDIA Laboratories).

Microwave-assisted synthesis of guar gum grafted acrylic acid superabsorbent polymer

Synthesis of superabsorbent polymer (SAP) is carried out similar to previous work[28] with slight modification in microwave irradiation, where microwave oven (IFB, 20BC4) is used instead of microwave reactor (Enerzi microwave systems, Belgaum, India). About 1 g of guar gum powder was dissolved in 100 mL of distilled water. Exactly 6 mL of acrylic acid is added, followed by 90 mL of ammonium persulphate (APS), which acts as an

initiator, and 90 mL of methylene bis acrylamide (MBA), which acts as a crosslinker with continuous stirring. The reaction mixture was subjected to microwave irradiation for 2.5 minutes at 70ºC. It was cooled to room temperature. To avoid the toxic nature of acrylic acid, the mixture was neutralised using 1N NaOH till the pH reached 7. The mixture was then precipitated using acetone. The precipitate obtained was kept for drying in a hot air oven for 5-6 hours at 60ºC.

Optimisation of parameters

Series of GG-g-AA SAPs were synthesised with varied concentrations of parameters such as concentration of monomer, initiator, crosslinker, and reaction time. The optimum value was obtained at the maximum grafting percentage. The grafting percentage was calculated using Eq. (1). Similar work was observed by Sutirman *et al.* in the synthesis of polymethacrylamide grafted chitosan via free radical polymerization[29].

$$\text{Grafting percentage} = \frac{(Weight\ of\ grafted\ superabsorbent - Weight\ of\ guar\ gum)}{Weight\ of\ guar\ gum} * 100 \quad \ldots (1)$$

The effect of the crosslinker was optimised for the highest percentage of swelling. About 10 mL of water was added to 1.0±0.1 g of powder sample and allowed to swell for 120 min. The weight of the swollen sample was noted. Equilibrium swelling was calculated using Eq. (2)

$$\text{Equilibrium swelling} = \frac{(Weight\ of\ swollen\ sample - Weight\ of\ dry\ sample)}{Weight\ of\ dry\ sample} * 100 \quad \ldots (2)$$

Fourier Transform Infrared Spectroscopy

Fourier Transform Infrared (FTIR) Spectroscopic analysis of guar gum and guar gum grafted acrylic acid SAP was performed using FTIR spectroscope (Thermo Scientific - Nicolet) between 400 to 4000 cm^{-1}. Sample preparation includes finely powdered SAP (~ 10 μ) mixed with potassium bromide (KBr) powder. Sample percentage in a mixture was desirable between 5–10% for best results.

Scanning Electron Microscopy

Scanning Electron Microscopy was carried out to study the morphology of guar gum grafted acrylic acid superabsorbent polymer and encapsulated beads using Scanning Electron Microscope (VEGA3 TESCAN). Samples were gold sputtered for conductivity.

***C. sinensis* peel sample collection and preparation**

C. sinensis (sweet oranges) was purchased in South Bengaluru where it was imported from Ananthapuram, Andhra Pradesh. Sweet orange fruits were peeled carefully to separate fruit, peel and fibres. *C. sinensis* peel was washed and dried in sunlight. Dried peel was powered using a table top domestic flour mill. The peel powder was sieved through 60 mesh.

Aqueous extraction of *C. sinensis* peel extract

Solid-liquid extraction was initiated by mixing *C. sinensis* peel powder with water in a ratio of 1:10. It was kept for continuous stirring for 48 hours[30]. The extract was filtered using Whatman filter paper No. 1. The residue was re-extracted following the same procedure. The extract obtained was allowed to settle if any residue present would get settled at the bottom. It was refiltered using Whatman filter paper No. 1, and the extract obtained was dried by evaporation of the solvent. The extract was stored at 4□. The weight of the extract was measured to obtain the yield of extraction. Yield of Extraction was calculated using Eq. (3)

$$\text{Yield of extraction} = \frac{(Weight\ of\ dried\ extract)}{(Weight\ of\ dry\ orange\ peel\ powder)} * 100 \quad \ldots (3)$$

Phytochemical analysis of *C. sinensis* peel extract

Phytochemical analysis was carried out to identify the bioactive present in the extract by a similar protocol followed by Arora *et al*. in their work on phytochemical screening of *C. sinensis* peel and pulp[31].

Test for flavonoids (Alkaline reagent test)

To 0.2 mL *C. sinensis* peel extract, 0.1 N sodium hydroxide solution was added. The solution turned deep yellow or *C. sinensis* colours, which indicated the presence of flavonoids.

Test for tannins (Braymer's test)

Exactly 0.2 mL *C. sinensis* peel extract was diluted to 2 mL using distilled water, to which a pinch of ferric chloride was added. A dark green colour solution obtained indicated the presence of tannins in the obtained extract.

Test for proteins

4% sodium hydroxide was added to 3 mL of *C. sinensis* peel extract, followed by a few drops of

1% copper sulphate solution. The solution turned to pink or violet, indicating the presence of proteins.

Test for saponins (Froth test)

Exactly 1 mL of *C. sinensis* peel extract was diluted to 10 mL using distilled water. The sample was boiled for 5 minutes and cooled. It was filtered using Whatman filter paper. 2.5 mL of filtrate was taken in a test tube to which 10 mL distilled water was added; it was shaken for 30 seconds and allowed to stand. A honeycomb-like froth formed, indicating the presence of saponins.

Test for reducing sugar (Benedict's test)

A small amount of Benedict's reagent was added to 2 mL of *C. sinensis* peel extract. The solution turned blue. It was allowed to stand for 10 minutes. Change in colour from blue to dark red or brown indicated the presence of reducing sugar.

Test for terpenoids (Salkowski's test)

To 5 mL of *C. sinensis* peel extract, 2 mL of chloroform was added, followed by a few drops of concentrated sulphuric acid. It formed a phase separation layer, and the formation of a reddish-brown ring at the interface indicated the presence of terpenoids.

Microencapsulation of *C. sinensis* peel extract - Preparation of beads

Microencapsulation of OPE was carried out using the coacervation phase separation technique[32]. A similar protocol of coacervation phase separation technique was followed, as mentioned by Stassen *et al.* in their study on protein encapsulation by poly (lactide-co-glycolide)[33]. The grafted superabsorbent polymer was dissolved in water, followed by a known quantity of *C. sinensis* peel extract. The reaction mixture was stirred well and left to stand overnight to remove air bubbles. The above solution was then dropped into acetone using a 25 mL hypodermic syringe with a 1 mm diameter and constant stirring. The beads thus formed were then crosslinked using 1% (v/v) glutaraldehyde solution by stirring the beads in the solution. Later, the crosslinked beads were rinsed with distilled water and dried. Fig. 1a and b showed wet encapsulated beads in acetone solvent and dried encapsulated beads, respectively.

Encapsulation efficiency

The content uniformity of *C. sinensis* peel extract for the beads was evaluated[34]. A known quantity of beads with *C. sinensis* peel extract was refluxed using hexane at 60°C. Refluxing initiates the extraction of *C. sinensis* peel extract from the superabsorbent polymer shell and continues till complete extraction of peel extract. Using a UV spectrophotometer, the absorbance of *C. sinensis* peel extract was recorded at 250 nm. Encapsulation efficiency was calculated using Eq. 4

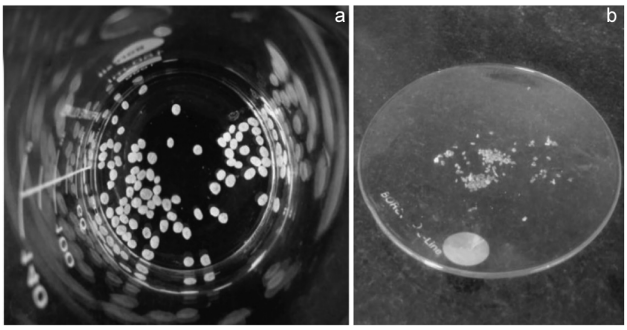

Fig. 1 — a) Encapsulated beads in acetone solvent; and b) Dried encapsulated beads.

$$\text{Encapsulation efficiency} = \frac{(Total\ concentration\ of\ OPE - Free\ concentration\ of\ OPE)}{(Total\ concentration\ of\ OPE)} * 100 \quad \ldots (4)$$

Release kinetics

Release kinetics plays a vital role in understanding the efficacy of the active component. Several models are developed to understand the pattern of release and factors affecting the release kinetics. The release kinetics of the beads containing *C. sinensis* peel extract was carried out by taking a known mass of beads in PBS and shaking them well. The absorbance of PBS containing *C. sinensis* peel extract is noted at definite time intervals at 250 nm wavelength. Further, the release model of *C. sinensis* peel extract from shell GG-g-AA SAP was analysed using various kinetic models like the Korseymeyer-Peppas model, the Higuchi model, Zero-order release kinetics, and First-order release kinetics.

Antimicrobial activity of encapsulated *C. sinensis* peel extract - Media preparation and inoculation

Nutrient Agar media was prepared by dissolving 28 g nutrient agar powder in 1000 mL of distilled water. The media was heated to a boil. It was sterilised by autoclaving at 15 psi pressure and 121℃. Sterilised media was cooled around 45℃, mixed well, and poured onto sterile Petri plates inside the sterilised laminar airflow chamber to avoid contamination. The bacterial culture of *Escherichia*

coli and *Bacillus subtilis* was spread onto the nutrient agar media by gliding the top of Petri plates. It was covered by paraffin and incubated at 40-45℃. The culture growth was observed between 24-48 hours[35].

Antimicrobial activity by well diffusion method

The agar well diffusion method was extensively used method to study the antimicrobial activity of plants or microbial extracts. A hole was bored on the inoculated Petri plates with a diameter of 6 to 8 mm using a sterile cork borer or a tip, and a known volume (20–100 µL) of the testing sample, i.e., SAP and OPE-e-SAP at the desired concentration was introduced into the well. Agar plates were incubated at 37-40℃. The antimicrobial solution gets diffused in the agar media to inhibit the growth of the micro-organism, which was observed between 24-48 hours[36].

Results and Discussion

Optimisation of reaction parameters for microwave-assisted synthesis of guar gum grafted acrylic acid superabsorbent polymer

The reaction parameters, such as reaction time, concentration of monomer, and initiator, were optimised for the highest grafting percentage.

Monomer (acrylic acid) optimisation was carried out by synthesising superabsorbent polymers with a series of different volumes of acrylic acid, i.e., from 2 to 8 mL. Fig. 2a depicts that the GG-g-AA superabsorbent with 6 mL of acrylic acid showed the highest grafting percentage; later, the plot maintained a constant trend. This behaviour was attributed to, initially, free radical sites being available abundantly; upon increasing the concentration of acrylic acid, the grafting percentage also increased. Once it reached equilibrium, homopolymers of acrylic acid were formed, which led to a decrease in the grafting percentage. A similar observation has been recorded by Biswal *et al.*[37] for the synthesis of carboxy methyl cellulose grafting with polyacrylamide.

Ammonium persulfate acts as the strong initiator in the polymerisation reaction. Initially, an increase in the concentration of the initiator led to an increase in the number of free radicals. Thus, the grafting percentage increased due to the high polymerisation rate. From Fig. 2b, maximum grafting of 90% was observed at 90 mg/mL concentration of ammonium persulfate. Above this level, grafting was unfavorable due to formation of large number of free radicals

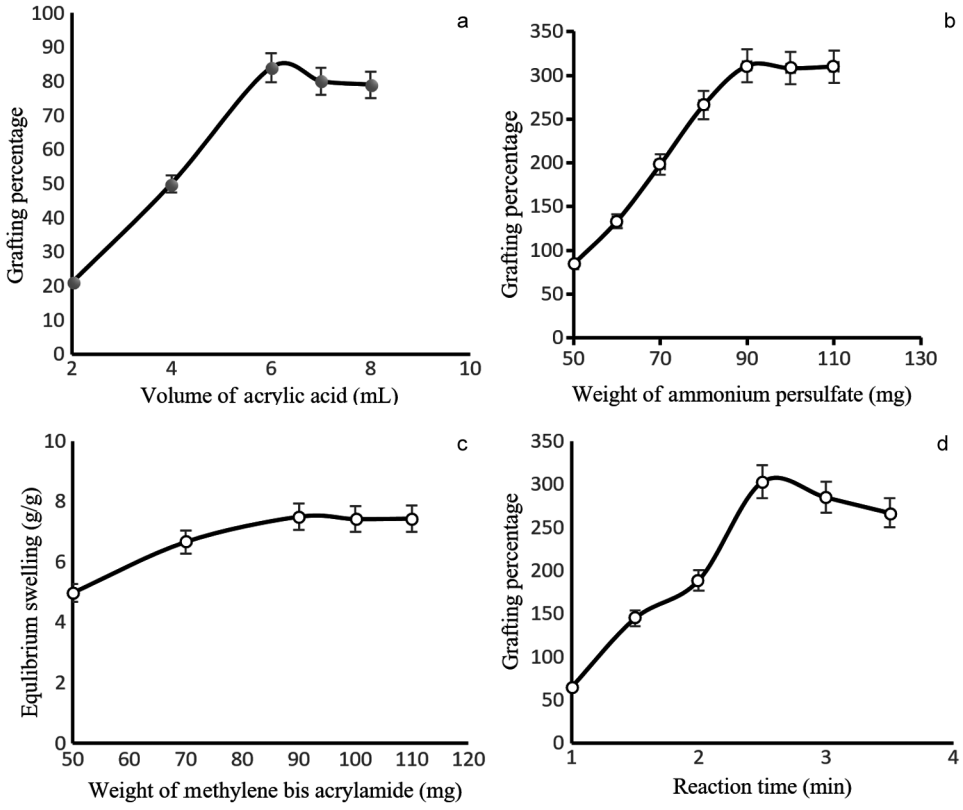

Fig. 2 — a) Effect of monomer (acrylic acid) on grafting percentage; b) Effect of initiator (APS) on grafting percentage; c) Effect of crosslinker on equilibrium swelling; and d) Effect of reaction time on grafting percentage.

which routed to shorter polymer chains. Identical results have been observed by Thakur *et al.*[38] for graft copolymerisation of the *Grewiaoptiva* plant, where potassium persulfate (KPS) was used as an initiator.

Crosslinker concentration influences the equilibrium swelling of the polymer. This characteristic feature relates to its capacity to form a three-dimensional network during polymerisation. Initially, as the concentration of crosslinkers increased, the equilibrium swelling also increased because the polymer network formed increased water penetration capacity. Higher equilibrium swelling of 7.5 g/g was observed at 90 mg/mL concentration of methylene bis acrylamide, as shown in Fig. 2c. At higher concentrations, with an increase in the crosslinking point, the density of the polymer network increases, which in turn reduces the water absorbency/selling capacity. Analogous results were obtained by Mudiyanselage *et al.* for their studies using N,N -methylene bisacrylamide as a crosslinker on highly absorbing acrylic acid-acrylamide-based superabsorbent polymer[39].

The time taken for irradiation of the microwave was considered as reaction time. When the microwave is irradiated on the sample, the atoms are excited, which speeds up the polymerisation reaction. From Fig. 2d at the outset, on increasing reaction rate, the grafting percentage increased drastically. At 2.5 minutes, the rate of reaction reached its peak value with 303% grafting percentage. Further increase in reaction time decreased grafting percentage. This reaction was attributed to the formation of short polymer chains due to the high availability of free atoms. Likitha *et al.* have deliberated similar observations upon microwave-assisted synthesis of guar gum-based SAP nanocomposite[40].

FTIR analysis

Fig. 3 represents FTIR spectra of pure guar gum and guar gum grafted acrylic acid superabsorbent polymer. The spectra depict a broad absorption band in the range of 3252–3575 due to the hydrogen-bonded OH stretch of the grafted copolymer. Followed by a series of spectra at 1661, 1000, and 815 confirms the presence of hydroxyl group (-OH) on the polysaccharide backbone[41]. Spectra at 2913 indicate vibration of axial deformation of C-H from a large number of methyl groups (CH_2). A sharp peak at 1662 indicates the C=O (carbonyl group) of amide and water. The peak at 1000 represents the single bond stretching of hydroxyl C-O from the C-O-C group[42]. This confirms the characteristic features of pure guar gum.

FTIR spectra of guar gum grafted acrylic acid SAP have a characteristic peak at 1418, confirming the stretch due to the carboxylic acid group of acrylic acid. The sharp peak at 1728 confirms the formation

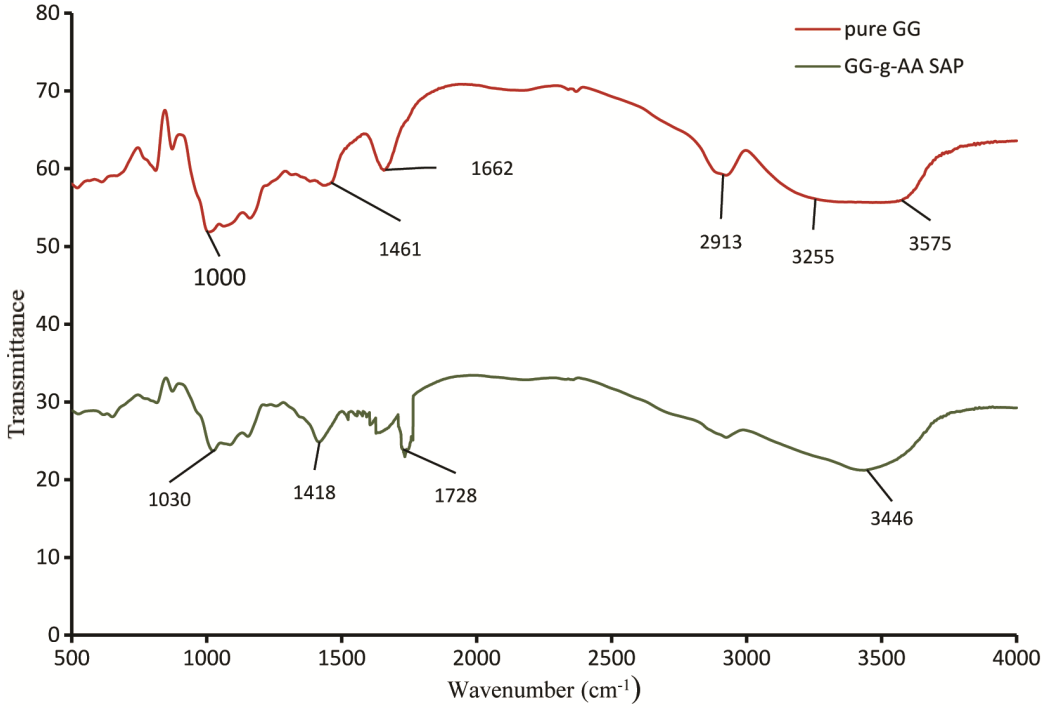

Fig. 3 — FTIR spectra of pure guar gum and guar gum grafted acrylic acid SAP.

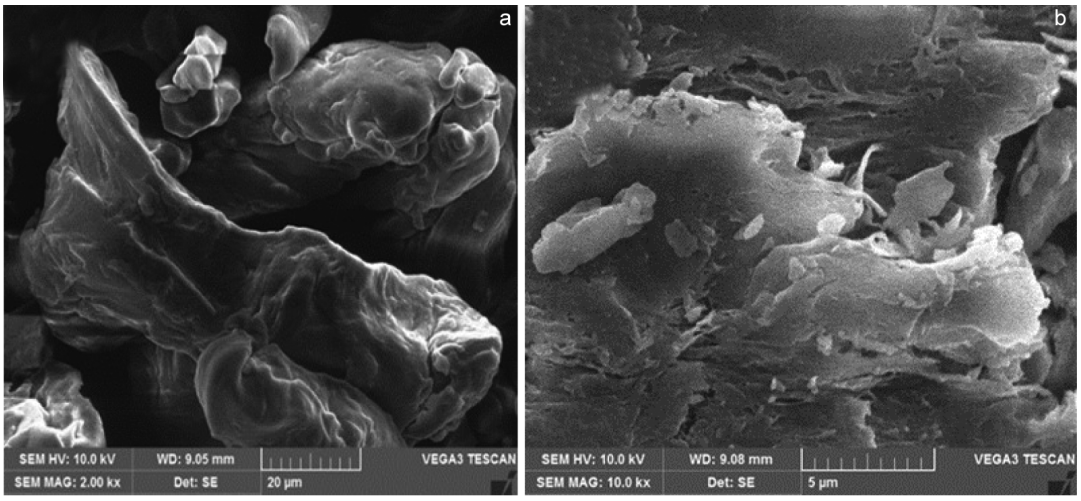

Fig. 4 — SEM micrographs a) pure guar gum; and b) guar gum grafted acrylic acid superabsorbent polymers.

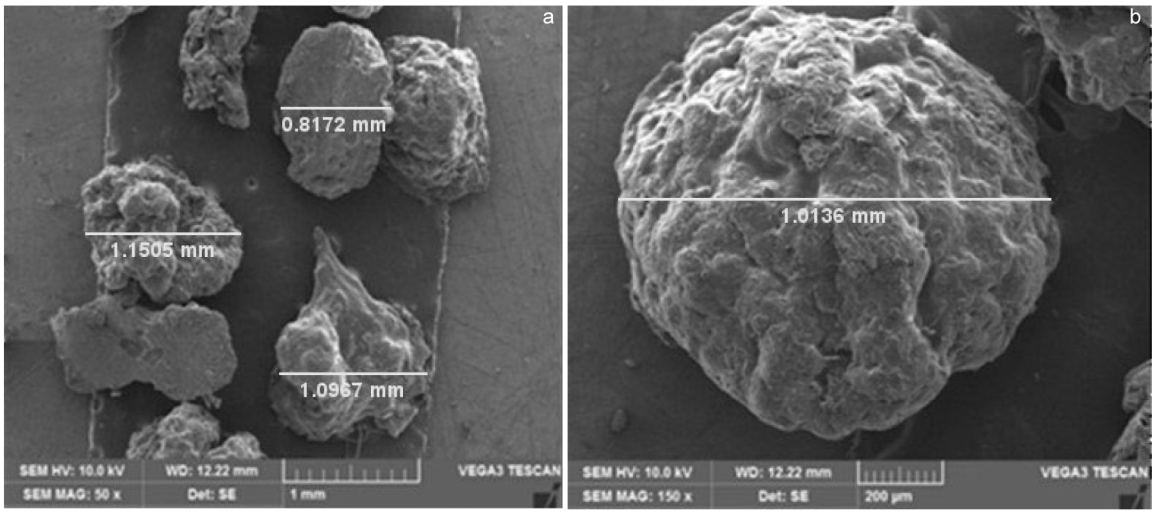

Fig. 5 — SEM micrographs of OPE encapsulated SAP beads at a) 50X magnification; and b) 150X magnification

of the ester group by the esterification reaction between acrylic acid and guar gum[43]. A peak at 3446 confirms OH vibrations due to the reaction between acrylic acid and guar gum. This confirms the grafting of an acrylic acid monomer onto the guar gum backbone.

SEM Morphology

SEM analysis of pure guar gum, GG-g-AA SAP, and encapsulated beads was carried out using a VEGA3 TESCAN electron microscope. Fig. 4a and b represent SEM images of pure guar gum and GG-g-AA SAP at 2kX and 10kX, respectively. Comparing the surface morphology between pure guar gum and GG-g-AA SAP, the latter with a highly porous surface confirms the grafting of acrylic acid onto guar gum backbone; similar observations are found by Sen *et al.* in their research on the synthesis and characterisation of novel flocculant-based polyacrylamide grafted carboxymethyl starch[44]. Fig. 5a and b at 50X and 150X, respectively, depict that beads formed are nearly spherical with a diameter of around 1 mm.

Phytochemical screening of *C. sinensis* peel extract

Aqueous extraction of *C. sinensis* peel resulted in a yield percentage of 10.8%. Upon performing a phytochemical analysis of *C. sinensis* peel extract, it ensued the presence of flavonoids, terpenoids, and saponins reduced sugar and tannins. It affirmed the absence of proteins in the extract obtained. Table 1 clearly illustrates the same. Similar observations are found in Gotmare *et al.* work[45].

Table 1 — Phytochemical analysis of *C. sinensis* peel extract

Phytochemicals	Result
Flavonoids	Positive
Terpenoids	Positive
Saponins	Positive
Protein	Negative
Reducing sugar	Positive
Tannins	Positive

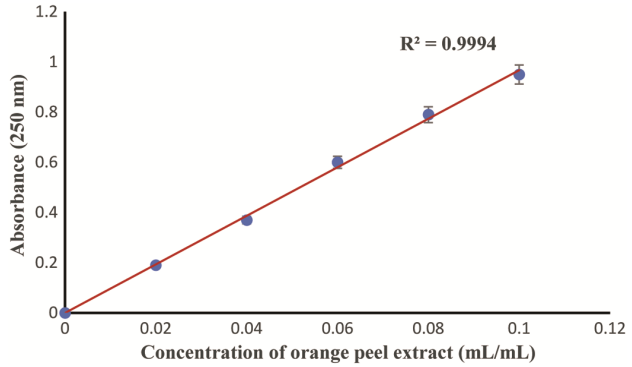

Fig. 6 — Standard calibration plot of *C. sinensis* peel extract.

Encapsulated bead size measurement

A digital vernier calliper was used to measure the size of beads formed from superabsorbent encapsulated with *C. sinensis* peel extract. For 50 beads, the average size was found to be 0.89 mm. The beads size range varies from 0.58 to 1.19 mm.

Encapsulation efficiency

The encapsulation efficiency of *C. sinensis* extract was evaluated using UV spectroscopy. Fig. 6 is the standard calibration for different concentrations of *C. sinensis* peel extract at 250 nm with R^2 value 0f 0.999. The total concentration of *C. sinensis* peel extract encapsulated was 0.154 mg/mL, and the release concentration was 0.115 mg/mL. The encapsulation efficiency of beads was calculated to be 74.6%. Similar results were obtained in the study of encapsulation and controlled release characteristics of crosslinked polyacrylamide particles by Sairam *et al.*[46].

Release kinetics of *C. sinensis* peel extract

Mathematical models studied for the release kinetics of *C. sinensis* peel extract are the Higuchi model, Korseymeyer-Peppas model, zero-order release kinetics and first-order release kinetics. The characteristic equations are as follows.

Korseymeyer-Peppas model (Power law): $\frac{M_t}{M_\infty} = k_p t^n$ (a)

Higuchi model: $\frac{M_t}{M_\infty} = k_H\sqrt{[t]}$ (b)

Zero order release kinetics: $C = C_0 - k_0 t$ (c)

First order release kinetics: $\frac{dC}{dt} = -k_1 C$ (d)

where M_t/M_∞ is the fraction of drug release at time t. C_0 and C are the initial and final concentrations of the drug, respectively. k_0, k_1, k_H and $k_p$are rate constant of zero order, first order, Higuchi model, and Korseymeyers-Peppas model, respectively.

Fig. 7 exhibits the relation between the drug release concentration vs reaction time. The results of equations (a) to (d) tabulated in Table 1 for n and rate constant values indicate that the release kinetics fits best for Zero order and the Korseymer-Peppas model best with an R^2 value of 0.999. This indicates that the release rate is independent of the concentration of the *C. sinensis* peel extract. The korseymeyer-Peppas model describes the release of the active components from a polymeric system. This empirical equation analyses both fickian and non-fickian release of drugs. In this casen=1.09, n value >1 indicates that the drug transport mechanism follows super case II transport, and the drug release mechanism is through relaxation associated with state transition and stress via water-swellable hydrophilic polymers, and geometry is thin planar film. The core GG-g-AA super absorbent polymer material is a water-swellable glassy hydrophilic polymer, which proves that the release of *C. sinensis* peel extract follows the Korsemeyer-Peppas model[47].

Antimicrobial studies

The antimicrobial activity of *C. sinensis* peel extract and encapsulated GG-g-AA SAP is tested using the agar well diffusion method against *E. coli* and *B. subtilis*, a gram-negative and gram-positive bacterium, respectively. Fig. 8 illustrates that the zone of inhibition is higher for *C. sinensis* encapsulated GG-g-AA SAP than for *C. sinensis* extract alone. This indicates that due to encapsulation, the release is sustainable, which is why the active component exhibited higher antimicrobial activity. Comparative data from Fig. 9 can be interpreted as a zone of inhibition for the gram-positive bacteria being higher than that of gram-negative bacteria in both cases. Similar observations were found by Dubey *et al.* in evaluating the antibacterial activity of methanolic and hydroethanolic extracts of sweet orange peels[48].

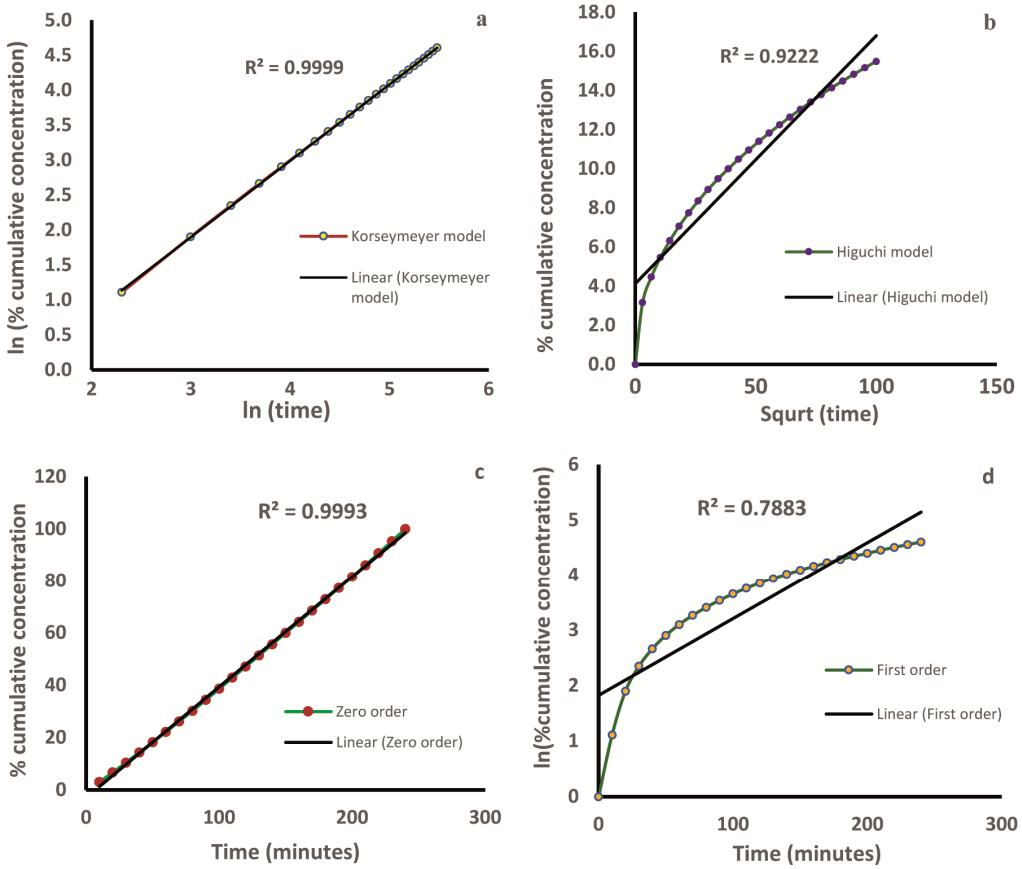

Fig. 7 — Release kinetics of encapsulated *C. sinensis* by a) Korseymeyer model; b) Higuchi model; c) Zero order release kinetics; and d) First order release kinetics.

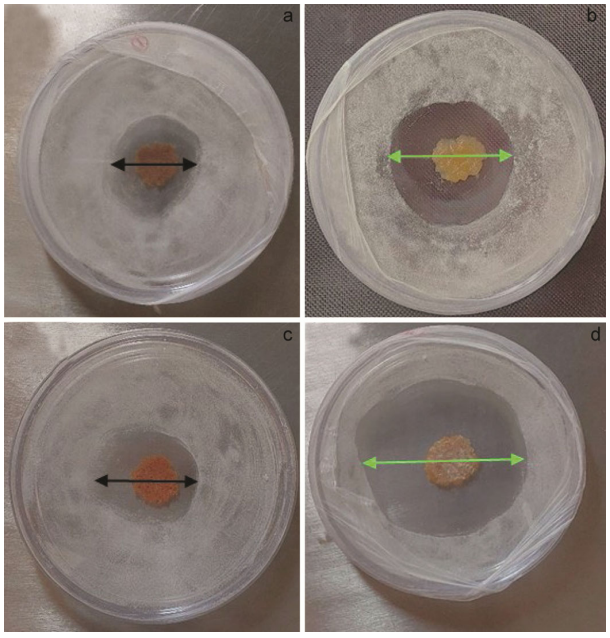

Fig. 8 — Zone of inhibition a) E. coli *by* C. sinensis *extract; b)* E. coli *by* C. sinensis *encapsulated GG-g-AA SAP; c) B. subtilis* by C. sinensis *extract; and* d) *B. subtilis* by C. sinensis *encapsulated GG-g-AA SAP.*

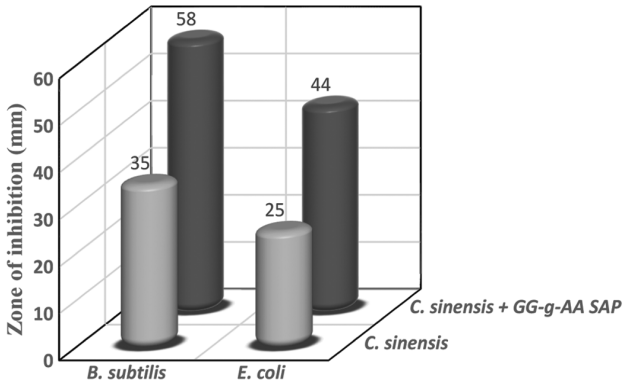

Fig. 9 — Comparison of zone of inhibition of *E. coli* and *B. subtilis* between *C. sinensis* and *C. sinensis* encapsulated GG-g-AA SAP.

Conclusion

Guar gum grafted acrylic acid superabsorbent polymer was synthesized using the microwave irradiation grafting technique. Reaction parameters were optimised at a higher grafting percentage. Characterisation via FTIR spectra and SEM morphology of GG-g-AA SAP proves the successful grafting of a monomer onto the guar gum backbone.

C. sinensis peel extract is obtained by conventional aqueous cold extraction method with a yield percentage of 10.8%. Phytochemical tests prove the presence of flavonoids, terpenoids, saponins, tannins and reducing sugar. Encapsulation of *C. sinensis* peel extract with synthesized GG-g-AA SAP was accomplished by the coacervation phase separation technique. It resulted in encapsulation efficiency of 74.6%. SEM analysis of encapsulated beads illustrated that to be round with ≈1mm diameter. Release kinetics hold good for Korseymeyer model and Zero order release kinetics with R^2 of 0.9999 and 0.9993 respectively. The befitting models rationalised that the release of active components is case II transport with erosion transport. Antimicrobial analysis of *C. sinensis* peel extract and encapsulated GG-g-AA SAP was performed for gram-negative *E.coli* and gram-positive *B.subtilis* bacteria. Results outlined that the zone of inhibition was higher for *C. sinensis* encapsulated GG-g-AA SAP compared to *C. sinensis* alone in both cases. It was found that the zone of inhibition was higher for gram-negative than that of gram-positive bacteria. Thus, it was concluded that *C. sinensis* encapsulated GG-g-AA SAP exhibited a higher potential to inhibit bacterial growth due to its sustainable release. This resulted in a sustainable product that finds application in fields like the cosmetic, pharmaceutical, and food industries.

Conflict of interest

The authors declare that there is no conflict of interest.

References

1 Nazzaro F, Orlando P, Fratianni F and Coppola R, Microencapsulation in food science and biotechnology, *Curr Opin Biotechnol*, 2012, **23**, 182-186, doi: 10.1016/j.copbio.2011.10.001.

2 Salmons B and Gunzburg W H, Therapeutic application of cell microencapsulation in cancer, In *Therapeutic Applications of Cell Microencapsulation*, J L Pedraz, G Orive, eds, (Springer New York), 2010, 92-103, doi: 10.1007/978-1-4419-5786-3_9.

3 Gimeno M, An overview of the latest development of microencapsulation for agricultural products, *J Environ Sci Health B*, 1996, **31**, 407-420, doi: 10.1080/03601239609373001.

4 Obeidat W M, Recent patents review in microencapsulation of pharmaceuticals using the emulsion solvent removal methods, *Recent Pat Drug Deliv Formul*, 2009, **3**, 178-192, doi: 10.1208/s12249.

5 Carvalho I T, Estevinho B N and Santos L, Application of microencapsulated essential oils in cosmetic and personal healthcare products - A review, *Int J Cosmet Sci*, 2016, **38**, 109-119, doi: 10.1111/ics.12232.

6 Saroglu O, Tav B, Yildirim R M and Karadag A, Microencapsulation of olive mill wastewater in Saccharomyces cerevisiae cells by spray drying and in vitro bioaccessibility of phenolic compounds, *Food Funct*, 2023, **14**, 3746-3759, doi: 10.1039/D2FO03872B.

7 Rama D, Shami T C and Bhasker R K U, Microencapsulation technology and application, *Def Sci J*, 2009, **59**, 82-95, doi: 10.14429/dsj.59.1489.

8 Krupla I, Nógellová Z, Špitalský Z, Janigová I, Boh B, *et al.*, Phase change materials based on high-density polyethylene filled with microencapsulated paraffin wax, *Energy Convers Manag*, 2014, **87**, 400-409, doi: 10.1016/j.enconman.2014.06.061.

9 Jo H J, Park K M, Na J H, Min S C, Park K H, *et al.*, Development of anti-insect food packaging film containing a polyvinyl alcohol and cinnamon oil emulsion at a pilot plant scale, *J Stored Prod Res*, 2015, **61**, 114-118, doi: 10.1016/j.jspr.2015.01.005.

10 Aziz T, Farid A, Haq F, Kiran M, Ullah A, *et al.*, A Review on the modification of cellulose and its applications, *Polymers (Basel)*, 2022, **14**, 3206-3240, doi: 10.3390/polym14153206.

11 Chen Q, Yu H, Wang L, Abdin Z, Chen Y, *et al.*, Recent progress in chemical modification of starch and its applications, *RSC Adv*, 2015, **5**, 67459-67474, doi: 10.1039/c5ra10849g.

12 Zhang L M, Zhou J F and Hui P S, A comparative study on viscosity behavior of water-soluble chemically modified guar gum derivatives with different functional lateral groups, *J Sci Food Agric*, 2005, **85**, 2638-2644, doi:10.1002/jsfa.2308.

13 Eyley S and Thielemans W, Surface modification of cellulose nanocrystals, *Nanoscale*, 2014, **6**, 7764-7779, doi: 10.1039/c4nr01756k.

14 Russell K E, *Free Radical Graft Polymerization and Copolymerization at Higher Temperatures,* www.elsevier.com/locate/ppolysci.

15 Food and Agriculture Organization, Citrus Fruit Statistical Compendium, Rome, 2020.

16 Pateiro M, Gómez B, Munekata P E S, Barba F J, Putnik P, *et al.*, Nanoencapsulation of promising bioactive compounds to improve their absorption, stability, functionality and the appearance of the final food products, *Molecules*, 2021, **26**, 1547-1553, doi: 10.3390/molecules26061547.

17 Geraci A, Di Stefano V, Di Martino E, Schillaci D and Schicchi R, Essential oil components of orange peels and antimicrobial activity, *Nat Prod Res*, 2017, **31**, 653-659, doi: 10.1080/14786419.2016.1219860.

18 Hegazy A E and Ibrahium M I, Antioxidant activities of orange peel extracts, *World Appl Sci J*, 2012, **18**, 684-688, doi: 10.5829/idosi.wasj.2012.18.05.64179.

19 M'hiri N, Veys-Renaux D, Rocca E, Ioannou I, Boudhrioua N, *et al.*, Corrosion inhibition of carbon steel in acidic medium by orange peel extract and its main antioxidant compounds, *Corros Sci*, 2015, **102**, 55-62, doi: 10.1016/j.corsci.2015.09.017.

20 Ezeonu F C, Chidume G I and Udedi S C, Insecticidal properties of volatile extracts of orange peels, *BioresourTechnol*, 2001, **76**, 273-274, doi: doi: 10.1016/S0960-8524(00)00120-6.

21 Oikeh E I, Oviasogie F E and Omoregie E S, Quantitative phytochemical analysis and antimicrobial activities of fresh

and dry ethanol extracts of *Citrus sinensis* (L.) Osbeck (sweet Orange) peels, *Clin Phytosci*, 2020, **6**, 46-52, doi: 10.1186/s40816-020-00193-w.

22 Doan Thi T U, Nguyen T T, Thi Y D, Ta Thi K H, Phan B T, *et al.*, Green synthesis of ZnO nanoparticles using orange fruit peel extract for antibacterial activities, *RSC Adv*, 2020, **10**, 23899-23907, doi: 10.1039/d0ra04926c.

23 Chudzikowski R J, Guar Gum and Its Applications, *J Soc Cosmet Chem*, 1971, **22**, 43-60.

24 Kaith B S, Sharma R and Kalia S, Guar gum based biodegradable, antibacterial and electrically conductive hydrogels, *Int J Biol Macromol*, 2015, **75**, 266-275, doi: 10.1016/j.ijbiomac.2015.01.046.

25 Thimma R T and Tammishetti S, Study of complex coacervation of gelatin with sodium carboxymethyl guar gum: microencapsulation of clove oil and sulphamethoxazole, *J Microencapsul*, 2003, **20**, 203-210, doi: 10.3109/02652040309178062.

26 Ghasemi S, Assadpour E, Kharazmi M S, Jafarzadeh S, Zargar M, *et al.*, Encapsulation of orange peel oil in biopolymeric nanocomposites to control its release under different conditions, *Foods*, 2023, **12**, 831-848, doi: 10.3390/foods12040831.

27 Savic I M, Savic Gajic I M, Milovanovic M G, Zerajic S and Gajic D G, Optimisation of ultrasound-assisted extraction and encapsulation of antioxidants from orange peels in alginate-chitosan microparticles, *Antioxidants*, 2022, **11**, 297-315, doi: 10.3390/antiox11020297.

28 Shruthi S B, Bhat C, Bhaskar S P, Preethi G and Sailaja R R N, Microwave assisted synthesis of guar gum grafted acrylic acid/nanoclay superabsorbent composites and its use in crystal violet dye absorption, *Green Sustain Chem*, 2016, **06**, 11-25, doi: 10.4236/gsc.2016.61002.

29 Sutirman Z A, Sanagi M M, Abd Karim K J and Wan Ibrahim W A, Preparation of methacrylamide-functionalized crosslinked chitosan by free radical polymerisation for the removal of lead ions, *Carbohydr Polym*, 2016, **151**, 1091-1099, doi: 10.1016/j.carbpol.2016.06.076.

30 Aguilera J M, Solid-liquid extraction, *Extraction Optimisation in Food Engineering*, 1st Edition, (CRC Press), 2003, 33-52.

31 Arora M and Kaur P, Phytochemical screening of orange peel and pulp, *Int J Res Eng Technol*, 2013, **2**, 517-22.

32 Kas H S and Oner L, Microencapsulation using coacervation/phase separation: An overview of the technique and applications, Wise DL, ed. In *Handbook of Pharmaceutical Controlled Release Technology*, (CRC Press), 2000, 301-326.

33 Stassen S, Nihant N, Martin V I, Grandfils C, Jerome R, *et al.*, Microencapsulation by coacervation of poly (lactide-co-glycolide): 1. Physico-chemical characteristics of the phase separation process, *Polymer (Guildf)*, 1994, **35**, 778-785, doi: 10.1016/0032-3861(94)90876-1.

34 Jyothi N V N, Prasanna P M, Sakarkar S N, Prabha K S, Ramaiah P S, *et al.*, Microencapsulation techniques, factors influencing encapsulation efficiency, *J Microencapsul*, 2010, **27**, 187-197, doi: 10.3109/02652040903131301.

35 Hall S, Hobson D, Lowe A and Paul W, Cultural studies, *Culture Media Language*, 1980, 285-291, doi: 10.4324/9780203381182.

36 Chaman S, Sharma G, Shalini and Reshi A K, Study of antimicrobial properties of *Catharanthus roseus* by agar well diffusion method, *Int Res J Pharm Appl Sci*, 2013, **3**, 65-68.

37 Biswal D R and Singh R P, Characterisation of carboxymethyl cellulose and polyacrylamide graft copolymer, *Carbohydr Polym*, 2004, **57**, 379-387, doi: 10.1016/j.carbpol.2004.04.020.

38 Thakur V K, Thakur M K and Gupta R K, Graft copolymers of natural fibers for green composites, *Carbohydr Polym*, 2014, **104**, 87-93, doi: 10.1016/j.carbpol.2014.01.016.

39 Mudiyanselage T K and Neckers D C, Highly absorbing superabsorbent polymer, *J Polym Sci A Polym Chem*, 2008, **46**, 1357-1364, doi: 10.1002/pola.22476.

40 Likhitha M, Sailaja R R N, Priyambika V S and Ravibabu M V, Microwave assisted synthesis of guar gum grafted sodium acrylate/cloisite superabsorbent nanocomposites: Reaction parameters and swelling characteristics, *Int J Biol Macromol*, 2014, **65**, 500-508, doi: 10.1016/j.ijbiomac.2014.02.008.

41 Nandiyanto A B D, Oktiani R and Ragadhita R, How to read and interpret ftir spectroscope of organic material, *Indonesian J Sci Technol*, 2019, **4**, 97-118, doi: 10.17509/ijost.v4i1.15806.

42 Balan V, Mihai C T, Cojocaru F D, Uritu C M, Dodi G, *et al.*, Vibrational spectroscopy fingerprinting in medicine: From molecular to clinical practice, *Materials*, 2019, **12**, 2884-2924, doi: 10.3390/ma12182884.

43 Srivastava A and Kumar R, Synthesis and characterization of acrylic acid-g-(-Carrageenan) copolymer and study of its application, *Int J Carbohydr Chem*, 2013, **2013**, 1-8, doi: 10.1155/2013/892615.

44 Sen G, Kumar R, Ghosh S and Pal S, A novel polymeric flocculant based on polyacrylamide grafted carboxymethyl starch, *Carbohydr Polym*, 2009, **77**, 822-831, doi: 10.1016/j.carbpol.2009.03.007.

45 Sulekha G and Jaya G, Orange Peel: A potential source of phytochemical compounds, *Int J Chemtech Res*, 2018, **11**, 240-243, doi: 10.20902/ijctr.2018.110229.

46 Sairam M, Babu V R, Naidu B V K and Aminabhavi T M, Encapsulation efficiency and controlled release characteristics of crosslinked polyacrylamide particles, *Int J Pharm*, 2006, **320**, 131-136, doi: 10.1016/j.ijpharm.2006.05.001.

47 Padmaa P M, Ani J P, Setty C M and Christoper G V P, Release kinetics-concepts and applications, *Int J Pharm Res Technol*, 2018, **8**, 12-20, doi: 10.31838/ijprt/08.01.02.

48 Dubey D, Dubey D, Balamurugan K, Agrawal R C, Verma R, *et al.*, Evalution of antibacterial and antioxidant activity of methanolic and hydromethanolic extract of sweet orange peels, *Recent Res Sci Technol*, 2011, **3**, 22-25.